TECTONIC COMPLEXITY WITHIN VOLCANICALLY INFILLED CRATERS AND BASINS ON MERCURY. Paul K. Byrne[1], Christian Klimczak[1], David M. Blair[2], Sabrina Ferrari[3], Sean C. Solomon[1,4], Andrew M. Freed[2], Thomas R. Watters[5], and Scott L. Murchie[6]. [1]Department of Terrestrial Magnetism, Carnegie Institution of Washington, Washington DC, 20015, USA (pbyrne@dtm.ciw.edu); [2]Department of Earth, Atmospheric, and Planetary Sciences, Purdue University, West Lafayette, IN 47907, USA; [3]Dipartimento di Geoscienze, Università degli Studi di Padova, Padua, Italy; [4]Lamont-Doherty Earth Observatory, Columbia University, Palisades, NY 10964, USA; [5]Center for Earth and Planetary Studies, National Air and Space Museum, Smithsonian Institution, Washington DC, 20013, USA; [6]Johns Hopkins University Applied Physics Laboratory, Laurel, MD 20723, USA.

Introduction: The dominant form of tectonic deformation on Mercury is contractional. Extension is almost entirely restricted to impact craters and basins that host volcanic smooth plains [e.g., 1–4]. However, extensional and compressional tectonic landforms within those impact features vary enormously in structural complexity—from sets of graben that describe polygonal patterns in craters tens of kilometers in diameter [5] to collocated basin-radial, -circumferential, and -oblique graben and contractional wrinkle ridges within the 1,640-km-diameter Caloris basin [6].

Here we describe the progression in tectonic complexity from some of the smallest to the largest impact features on Mercury, together with the implications of recent numerical modeling for the Caloris basin in particular, and for impact basin formation, tectonics, and volcanism on the innermost planet in general.

Impact crater/basin tectonics: We include map patterns for tectonic structures within four representative volcanically flooded impact features on Mercury: (a) a "ghost crater," (b) the Mozart basin, (c) the Rembrandt basin, and (d) the Caloris basin (**Fig. 1**).

(a) Ghost crater. Ghost craters are impact features that have been entirely covered by lavas, their presence marked by a ring of tectonic features localized above the buried crater rim [e.g., 2]. The crater in **Fig. 1a**, situated in the northern volcanic plains [7] and outlined by a ridge ring ~100 km in diameter, contains a set of graben with no strongly preferred orientations that divide the plains infill into polygonal blocks [3]. The graben extend from the crater center to ~0.8 its radius (r_{GC}). Contractional ridges external to the crater terminate at its peripheral ridge and do not penetrate the interior. This structural arrangement is characteristic of graben-bearing ghost craters, which primarily occur in the northern and circum-Caloris smooth plains [3,5].

(b) Mozart basin. The 235-km-diameter Mozart basin contains both graben and ridges, though these structures occur only within its peak ring [4] (**Fig. 1b**). Basin-circumferential graben form an annulus ~0.2–0.4 r_M concentric to the basin center. From this annulus to the peak ring at ~0.5 r_M, graben occur in a mix of basin-radial, -circumferential, and -oblique orientations. Ridges lie within the annular graben and show no preferred orientations. Structures are fewer in number in the southwestern sector of basin infill within Mozart's peak ring. This general tectonic pattern is also observed within the peak rings of the similarly sized Raditladi and Rachmaninoff basins [4].

(c) Rembrandt basin. This 715-km-diameter basin is riven along its northwestern interior by a northeast–southwest-trending 1,000-km-long fault array interpreted to be a fold-and-thrust belt (FTB) [6]. Apart from the FTB, however, the basin floor is heavily deformed by extensional and contractional structures [8,9] (**Fig. 1c**). Collocated basin-radial sets of graben and ridges form a fan-like pattern centered on the basin outward from ~0.2 r_R and are spatially bounded by circumferential ridges at ~0.5 r_R (and circumferential graben along the northern portion of the ridges). Local clusters of ridges without preferred orientations lie in the southwestern and eastern basin interior beyond ~0.5 r_R [9].

(d) Caloris basin. The largest impact basin recognized on Mercury also hosts the most tectonically deformed smooth plains on the planet, Caloris Planitia [6] (**Fig. 1d**). A basin-radial graben set, Pantheon Fossae [e.g., 1], the dominant extensional assemblage in the basin, originates from a point near the center and extends to ~0.55 r_C. Pantheon Fossae is bounded by circumferential graben that form a near-complete annulus from ~0.45 to 0.55 r_C. Outward, extension is manifest by basin-oblique graben that define a complex polygonal map pattern and steadily decrease in width, depth, and length towards the basin margin [6].

Basin-circumferential ridges are the most abundant type of contractional structure, and extend from ~0.1 to 0.7 r_C. Radially orientated ridges also occur within this zone but are less common than their Caloris-concentric counterparts. Outside ~0.7 r_C, ridges show no particular orientation preference and so also form a polygonal pattern that becomes less prominent toward 1.0 r_C [6].

Formation hypotheses: Almost every tectonically deformed impact structure on Mercury is characterized by a scarcity of definitive cross-cutting relations, challenging recognition of a developmental sequence for attendant structures. Where ridges and graben spatially coincide within ghost craters, their superposition relations are often unclear [3]; they do not coincide in Mozart at all [4]. Extensional structures appear to be superposed on, and so postdate, contractional landforms in Rembrandt and Caloris [e.g., 1], but no clear dip- or strike-slip offsets are observed in either basin.

However, finite-element modeling results for ghost craters [10] and mid-sized basins such as Mozart [4] may provide insight into the deformation that shaped Rembrandt and Caloris. Thermal contraction of thick, rapidly emplaced lava flows produces horizontal extensional stresses that favor the formation of mixed-orientation graben in volcanic plains, whereas horizontal shortening in response to cooling and contraction of the planet's interior or flexure due to volcanic loading was likely responsible for the formation of ridges in both ghost craters and Mozart basin [2,4,10]. Moreover, models of thermally contracting lavas also show that a buried basin ring strongly localizes radial extensional stress and circumferential graben formation [4].

Implications: Previous studies suggested that the prominent fossae within Caloris may have formed due to dike propagation [11] or to flexural uplift of the basin center, in response either to the volcanic emplacement of the circum-Caloris smooth plains [12] or to inward flow of the lower crust [13]. No extensive plains are observed exterior to Rembrandt [14], suggesting intrusive activity or inward crustal flow may be responsible for the fossae in at least that basin. Graben of mixed orientation in Caloris and Rembrandt may attest to near-isotropic horizontal extension of rapidly emplaced lavas; the decrease in graben size with increasing distance from the basin center likely indicates steadily reducing plains thickness [5,10] and thus original basin depth. If the pronounced circumferential graben within these basins reflect extension above a buried basin ring, Rembrandt and Caloris may be multi-ring basins—a class of impact feature not yet clearly documented for Mercury [15]. Finally, the ridges within these basins may primarily be the result of global contraction on Mercury. If so, the differences in orientation from basin-circumferential or -radial to -oblique could reflect a transition of the responsible stress field from strongly basin–shape-influenced to horizontally isotropic with increasing distance from basin center.

Informed by new tectonic maps of Caloris and Rembrandt (**Fig. 1**), these inferences can be tested numerically in the manner of recent models for ghost craters and basins [4,12], with the goal of reproducing the full range of tectonic complexity within flooded impact features on Mercury.

References: [1] Murchie S. L. et al. (2008) *Science*, *321*, 73. [2] Watters T. R. et al. (2009) *EPSL*, *285*, 309. [3] Watters T. R. et al. (2012) *Geology*, *40*, 1123. [4] Blair D. M. et al. (2013) *JGR*, *118*, in press. [5] Klimczak C. et al. (2012) *JGR*, *117*, E00L03. [6] Byrne P. K. et al. (2012) *LPS, 43*, abstract 1722. [7] Head J. W. et al. (2011) *Science*, *333*, 1853. [8] Watters T. R. et al. (2009) *Science*, *324*, 618. [9] Ferrari S. et al. (2012) *EPSC Abstracts*, *7*, abstract 2012-874. [10] Freed A. M. et al. (2012) *JGR*, *117*, E00L06. [11] Head J. W. et al. (2008) *Science*, *321*, 69. [12] Freed A. M. et al. (2009) *EPSL*, *285*, 320. [13] Watters T. R. et al. (2005) *Geology*, *33*, 669. [14] Denevi B. D. et al. (2012) *EPSC Abstracts*, *7*, abstract 2012-812. [15] Fassett, C. I. et al. (2012), *JGR*, *117*, E00L08.

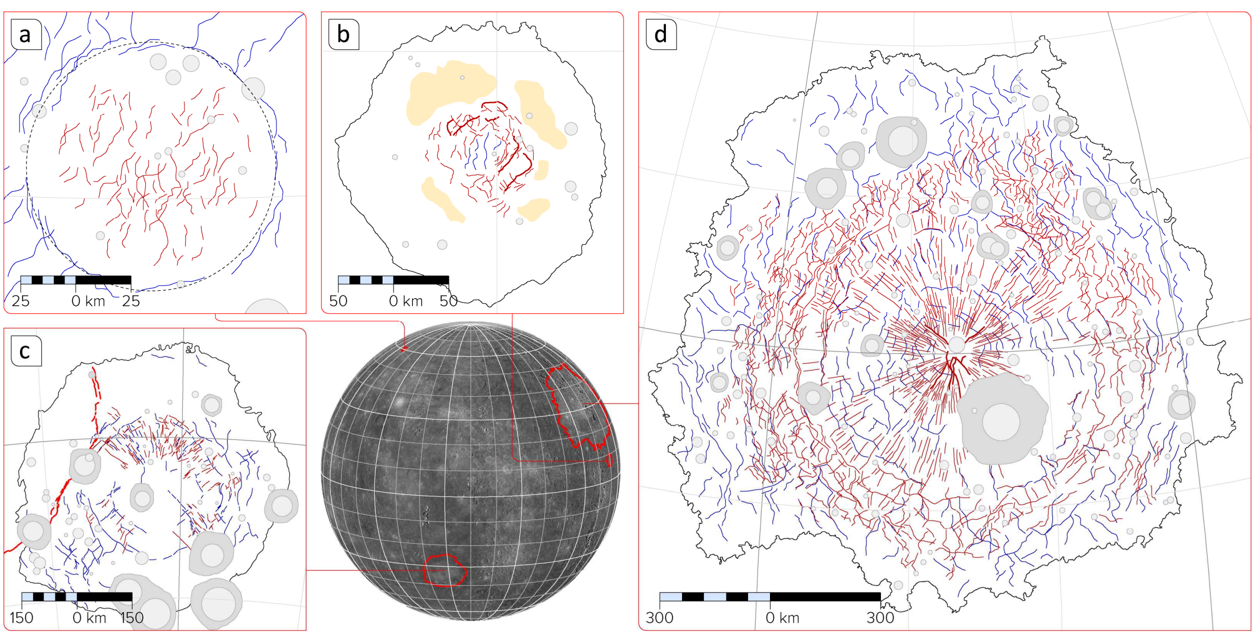

Figure 1. Structural sketch maps of exemplar flooded impact features.(a) Ghost crater; (b) Mozart basin; (c) Rembrandt basin (after [9]); and (d) Caloris basin. Orthographic projections centered at: (a) 60.3°N, 36.7°E; (b) 7.8°N, 169.6°E; (c) 33.5°S, 88°E; and (d) 30°N, 161°E. Sketches feature graben (dark red lines), ridges (dark blue), superposed craters and ejecta (light and dark grey), and Mozart peak ring (sand).